Composites Part B 89 (2016) 108–116

Contents lists available at ScienceDirect

Composites Part B

journal homepage: www.elsevier.com/locate/compositesb

Effect of Cu-doped graphene on the flammability and thermal properties of epoxy composites

Yun Liu [a, b], Heeralal Vignesh Babu [b], Jianqing Zhao [c], Asier Goñi-Urtiaga [d], Raquel Sainz [d], Rafael Ferritto [d], Marcos Pita [e], De-Yi Wang [b, *]

[a] College of Chemistry and Chemical Engineering, Wuhan Textile University, Fangzhi Road, 1, Wuhan 430073, PR China
[b] IMDEA Materials Institute, C/Eric Kandel, 2, Getafe, Madrid 28906, Spain
[c] School of Materials Science and Engineering, South China University of Technology, Guangzhou 510006, PR China
[d] Nanoinnova Technologies S.L., Parque Científico de Madrid, C/Faraday 7, Madrid 28049, Spain
[e] Instituto de Catálisis y Petroleoquímica, CSIC, C/Marie Curie 2, Madrid 280409, Spain

ARTICLE INFO

Article history:
Received 23 September 2015
Received in revised form
18 November 2015
Accepted 25 November 2015
Available online 8 December 2015

Keywords:
A. Polymer–matrix composites (PMCs)
A. Hybrid
B. Thermal properties
E. Thermosetting resin
Flammability

ABSTRACT

Cu-doped graphene (graphenit-Cu) was successfully prepared through chemical reduction method, and its surface morphology, crystalline structure and Cu content in graphenit-Cu were characterized by scanning electron microscopy (SEM), X-ray diffraction (XRD), inductive couple plasma (ICP) and electrochemical cyclic voltammetry, respectively. Graphenit-ox/epoxy systems and graphenit-Cu/epoxy systems were prepared, and the contents of graphenit-ox and graphenit-Cu were kept as 1 and 3 wt%, respectively. The effect of graphenit-ox or graphenit-Cu on the flame retardancy, combustion properties, thermal degradation and thermomechanical properties of epoxy resin was investigated systematically by limiting oxygen index (LOI), cone calorimeter (Cone), thermogravimetric analysis (TGA) and dynamic mechanical analysis (DMA). Compared to graphenit-ox, the addition of graphenit-Cu reduced the heat release rate (HRR), total smoke production (TSP) and smoke production rate (SPR), and improved LOI values of epoxy composites. Moreover, the addition of graphenit-ox also had little flame retardant effect on epoxy composite. The possible synergistic effect between graphene and Cu was confirmed in the flame retardant epoxy composites. TGA and DMA results also indicated the considerable effect on the thermal degradation and thermomechanical properties of epoxy composites with the addition of graphenit-Cu. The results supplied an effective solution for developing excellent flame retardant epoxy composites.

1. Introduction

Epoxy resin (EP) has been widely utilized in a variety of fields, such as electronic/electrical insulation, laminates and composites, adhesives, and coatings, due to its outstanding properties such as high thermal stability, great versatility, good mechanical properties, strong adhesion, low shrinkage, chemical resistance and as an excellent solvent [1–4]. However, the high flammability of epoxy resin has hindered its application in some fields, especially in electronic/electrical insulation, laminates and composites. Thus, the research on flame retardant epoxy resin is increasingly attracting more attention [5–8]. There are two methods to improve the flame retardant properties of epoxy resin. In the first method, some flame retardants are physically added into epoxy resin [9–11]; and in the other method, some intrinsic flame retardant elements like P [3,12], Si [13], N [14] are grafted into the macromolecular chains through chemical reactions. An efficient and versatile method to prepare flame retardant epoxy composites is the physical addition method, but it is difficult to disperse the flame retardant homogeneously into epoxy resin. Alternatively, an intrinsic flame retardant epoxy resin provides better mechanical properties; however, their preparation process is more complicated.

During the past decade, one of the promising solutions to improve the flame retardant properties of epoxy resin is to incorporate nanoparticles as filler into epoxy resin [15]. Likewise, different kinds of nanomaterials, such as montmorillonite (MMT) [16], sepiolite [17], carbon nanotube (CNT) [6], or layered double

* Corresponding author. Tel.: +34 917871888.
E-mail address: deyi.wang@imdea.org (D.-Y. Wang).

http://dx.doi.org/10.1016/j.compositesb.2015.11.035
1359-8368/

hydroxide (LDH) [18] have been introduced into epoxy resin. These nanofillers have already showed interesting results on the flame retardant properties of epoxy composites. Recently, we have reported that functionalized LDH-based epoxy nanocomposites reached V-0 rating in the UL-94 vertical burning test with low loading functionalized LDH [18–20]. The introduction of these nanoparticles reduced the heat release rate (HRR) and simultaneously improved the mechanical properties of epoxy composites.

Since its discovery in 2004, graphene has attracted much attention due to its Young's modulus, fracture strength, specific surface, electron mobility and thermal conductivity [21–23]. These remarkable properties made graphene and its derivatives to be applicable in the field of batteries, sensors, electronic devices and hydrogen storage. Also graphene based nanofillers were utilized to improve the performance of polymers [24,25]. Due to its high thermal resistance, graphene behaved as an effective barrier which slowed down the heat/mass transfer during the combustion of polymer [22]. Based on this, further research was directed towards graphene and its derivatives as flame retardants to enhance the flame retardant behavior of polymeric materials [26–28]. The results indicated that the addition of graphene and its derivatives improved the flame retardant properties of polymeric materials [26–28]. However, the effect of Cu-doped graphene on the flame retardant properties of polymers is virtually not reported.

This paper describes the complete characterization of successfully synthesized Cu-doped graphene (graphenit-Cu) by using scanning electron microscopy (SEM), X-ray diffraction (XRD), Inductive couple plasma (ICP) and electrochemical cyclic voltammetry. Further, we report the preparation and characterization of graphenit-ox and graphenit-Cu based Epoxy composites; and their significant effect on the flame retardant properties, combustion properties, thermal degradation and thermomechanical properties of epoxy resin, are systematically studied using limiting oxygen index (LOI), cone calorimeter (Cone), thermogravimetric analysis (TGA) and dynamic mechanical analysis (DMA) techniques.

2. Experimental

2.1. Materials

Epoxy resin (L20) was purchased from Faserverbundwerkstoffe® Composite Technology, Germany and 4,4′-Diaminodiphenyl sulfone (DDS) was purchased from TCI Chemicals. Slightly oxidized graphene nanoplatelets (graphenit-ox) were supplied by Nanoinnova Technologies S. L. (Madrid, Spain), and Cu-doped graphene (graphenit-Cu) were prepared through chemical reduction method by Nanoinnova Technologies S. L. (Madrid, Spain).

2.2. Preparation of graphene based epoxy composites

A fixed weight fraction (1 and 3 wt%) of graphenit-ox and graphenit-Cu was added into epoxy resin to prepare epoxy composites. To obtain a favorable dispersion of graphenit-ox and graphenit-Cu into epoxy resin, a three-roll mill from EXAKT® 80E (Advanced Technologies GmbH, Germany) was used. In order to achieve better incorporation as well as dispersion of graphenit-ox or graphenit-Cu into epoxy resin, the whole suspension was milled two times for about 15 min. During the first time of mill, the gap between the feed roll and the apron roll was set to 90 and 20 μm, respectively and for the second time, it was adjusted to 60 and 20 μm, respectively. Then, the suspension in a beaker was heated to 125 °C in an oil bath. DDS was added slowly to the suspension and stirred for 15 min until DDS was totally dissolved. Subsequently, the suspension was placed into a vacuum oven at 110 °C for 10 min to drive off the bubbles and immediately poured into pre-heated (160 °C) silicon-rubber moulds and the curing procedure was set as follows: 160 °C for 2 h, 180 °C for 2 h and 200 °C for 1 h. Following the same procedure, epoxy resin, epoxy composites with 1 wt% and 3 wt% of graphenit-ox (1% and 3% graphenit-ox-epoxy), and epoxy composites with 1 wt% and 3 wt% of graphenit-Cu (1% and 3% graphenit-Cu-epoxy) were prepared.

2.3. Measurements

2.3.1. Limiting oxygen index test

LOI test was carried out with an oxygen index model instrument (Fire Testing Technology, UK), and sheet dimensions of the samples were 130 mm × 6.5 mm × 3.2 mm according to ASTM D2863-97.

2.3.2. Cone calorimeter test

The combustion behaviors of epoxy composites were investigated by a cone calorimeter (Fire Testing Technology, UK) according to the procedures in ISO 5660-1. Specimens with sheet dimensions of 100 mm × 100 mm × 3 mm were placed on aluminum foil and irradiated horizontally at a heat flux of 50 kW/m^2. Each sample was tested for three times.

2.3.3. Thermogravimetric analysis

Thermal stability of sample was studied on a Q50 Thermogravimetric Analyzer (TA Instruments, USA). The heating rate was set to 10 °C/min, and about 10 mg of the sample was tested under nitrogen with a flow rate of 90 mL/min from room temperature to 700 °C. The temperature of the instrument was reproducible to within ±1 °C, and the mass was reproducible to within ±0.1%.

2.3.4. Dynamic mechanical analysis

Thermomechanical properties of epoxy composites were examined by a Dynamic Mechanical Analyzer Q800 (TA Instruments, USA). The dimensions of sample were 35 mm × 10 mm × 2 mm. The samples were tested in a single cantilever clamp with a frequency of 1 Hz and an amplitude range of 15 μm at the heating rate of 3 °C/min from room temperature to 280 °C.

2.3.5. Scanning electron microscopy

Surface morphology and particle size of graphenit-Cu was characterized using a TM-1000 Tabletop Hitachi microscope. The sample was coated with a conductive gold layer and pasted on carbon conductive belt before SEM observation.

Morphologies of epoxy composites with 3% graphenit-ox and epoxy composites with 3% graphenit-Cu were acquired with focused ion beam-field emission gun scanning electron microscope (FIB-FEGSEM) dual-beam microscope (Helios Nano Lab 600i, FEI). All the samples were coated with a conductive gold layer and pasted on carbon conductive belt before FIB-FEGSEM observation.

2.3.6. X-ray diffractometer (XRD)

Crystallography of graphenit-Cu was investigated by a XPERT-PRO X-ray diffractometer. The Cu K_α (λ = 1.5406 Å) radiation source was operated at 45 kV and 40 mA with a scan speed of 2° min^{-1}.

2.3.7. Electrochemical cyclic voltammetry

Electrochemical cyclic voltammetry of graphenit-Cu was carried out in a three-electrode cell. Glassy carbon, Pt wire and Ag/AgCl in 3 M KCl (BASi) were used as working electrode, counter electrode and reference electrode respectively. All electrodes were introduced in a standard three-electrode cell containing 0.1 mol/L KOH (Scharlau) solution as electrolyte. Graphenit-Cu ink was prepared in milli-Q water with 15 wt% Nafion and the concentration of Graphenit-Cu was 5 mg mL^{-1}. 25 μL of the above ink was pippetted

onto the working electrode and dried at room temperature. Cyclic voltammograms were recorded at a scan rate of 20 mV s^{-1}. Electrochemical measurements were recorded using a μ-Autolab system (Metrohm Autolab).

2.3.8. Inductive couple plasma

The content of Cu in graphenit-Cu was investigated by using ICP-MS NexION 300XX (Perkin–Elmer).

2.3.9. Transmission electron microscopy (TEM)

A 200 KV JEOL 2100 transmission electron microscope was used for the analysis. The sample was prepared by adding a drop of diluted graphenit-Cu dispersed in ethanol on a lacey carbon-coated copper grid 200 Mesh and then let to dry.

3. Results and discussion

3.1. Preparation and characterization of Cu doped graphene

Cu-doped graphene (graphenit-Cu) was prepared by means of immobilization of Cu particles in graphenit-ox. Synthesis of graphenit-Cu was carried out through chemical reduction method, using graphenit-ox, $CuCl_2$ as copper metal precursor and $NaBH_4$ as a reducing agent, at room temperature and under inert atmosphere, as described elsewhere [29].

The surface morphology, crystalline structure and Cu content in graphenit-Cu were characterized by scanning electron microscopy (SEM), transmission electron microscopy (TEM), X-ray diffraction (XRD) and inductive couple plasma (ICP), respectively. From the SEM and TEM images of graphenit-Cu (Fig. 1), it was observed that the dispersion of Cu particles was homogeneous on the surface of graphenit-ox. This indicated that during the material synthesis, there was an optimum as well as numerous nucleations of copper metal particles.

XRD spectrum of graphenit-Cu is presented in Fig. 2. There was a well defined sharp diffraction peak at 26.5° and two small peaks at 54.5° and 78.1°, corresponding to (004), (002) and (110) crystallographic phases of slightly oxidized graphene (graphenit-ox) [30], respectively. The rest of the spectrum was complemented by a series of peaks which were attributed to a mixture of phases between metallic copper and its oxides [31]. Metallic Cu^0 exhibited three characteristic peaks at 43.2°, 50.3° and 73.4° corresponding to (111), (200) and (220) crystallographic phases, respectively. Peaks at 36.4°, 38.5°, 48.6° and 61.2° were matched well with the peaks of Cu^{II} oxidation state which is the most stable form of copper oxide

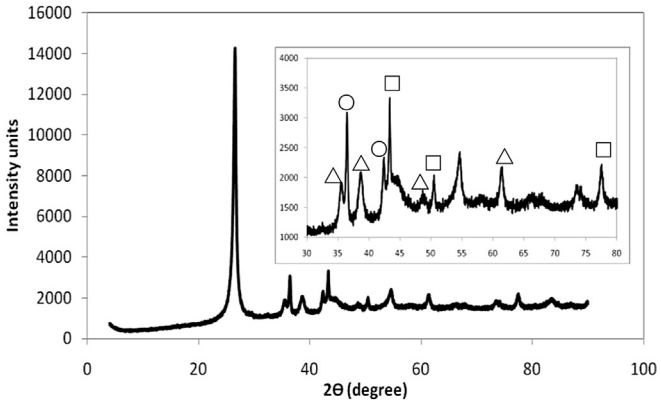

Fig. 2. XRD spectrum of graphenit-Cu, (□) Cu, (△) CuO and (○) Cu_2O.

(cupric oxide, CuO). In addition, two characteristic diffraction peaks of less stable Cu^I oxidation state (cuprous oxide, Cu_2O) were also found at 36.4° and 42.6°. These data confirmed the coexistence of several phases of metallic and copper oxides in graphenit-Cu.

From the induced coupled plasma (ICP) analysis, it was found that the content of Cu in graphenit-Cu was 9.0 wt%. This result was in good agreement with the 10 wt% loading obtained from the molar ratio of graphenit-ox and $CuCl_2$ in the synthesis process.

In order to confirm the presence of copper in the material and to estimate its mass ratio in graphenit-ox, graphenit-Cu was characterized by electrochemical cyclic voltammetry. Cyclic voltammograms of graphenit-ox and graphenit-Cu are depicted in Fig. 3. Cyclic voltammogram of bare graphenit-ox showed a characteristic capacitive behavior of graphitic materials with a well defined rectangular shape. This shape resulted from the double-layer effect, where the charges from electrolyte and electrode arranged in the surface of the electrode, providing electrostatic charge. It was noted that a pseudo-capacitance was provided by a redox couple with a former potential of 0.32 V vs. Ag/AgCl 3 mol/L KCl. This redox was attributed to the protonation/deprotonation of quinone groups in the material. The specific capacitance of graphenit-ox was calculated by integrating the area of the voltammograms and it was found to be 70 F g^{-1}. In case of graphenit-Cu, the capacitance was considerably reduced and a number of redox peaks appeared in the voltammogram. The decrease in double-layer capacitance was caused by a smaller mass of graphene in the electrode and also a modification on the double-layer capacitive properties of the functionalized graphene. The double-layer capacitance of

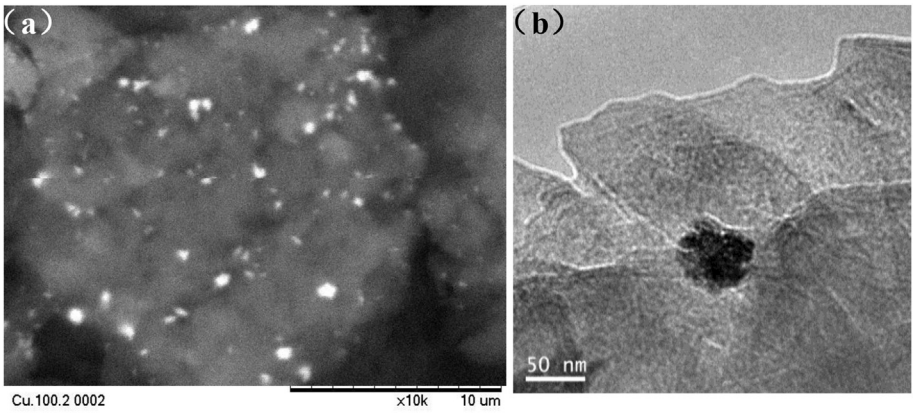

Fig. 1. SEM (a) and TEM (b) images of graphenit-Cu.

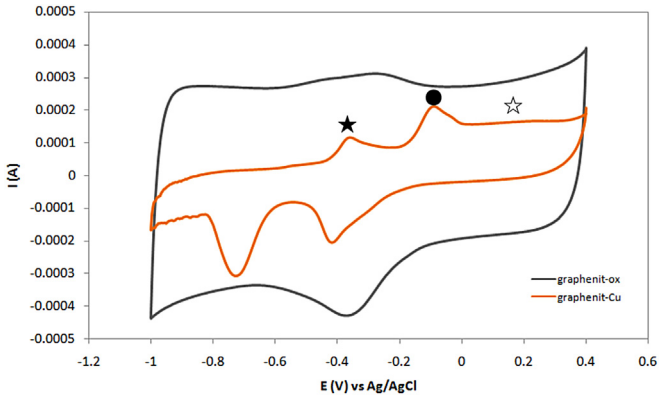

Fig. 3. Cyclic voltammograms of graphenit-ox and graphenit-Cu.

graphenit-Cu was calculated by extrapolating the anodic base-line from −1 to −0.6 V and the cathodic base-line from 0.3 to −0.1 V. The value obtained from the calculation was 27.5 F g^{-1}. Redox peaks were attributed to the oxidation and reduction of copper in alkali medium. The peaks corresponding to the following oxidation reactions were marked in Fig. 3 [32]:

$$(\bigstar)\quad 2\,Cu + 2\,OH^- \rightarrow Cu_2O + H_2O \tag{1}$$

$$(\bullet)\quad Cu_2O + 2\,OH^- \rightarrow 2\,CuO + H_2O \tag{2}$$

$$(\star)\quad CuO + H_2O \rightarrow Cu(OH)_2 \tag{3}$$

From the charge value of the oxidation peaks at −0.364 and −0.093 V, the electroactive mass of Cu was calculated, and the content of Cu was ca. 1.8 wt% in graphenit-Cu. This value corresponded to the electroactive mass of Cu. It meant that the amount of copper in contact with the electrolyte was able to carry out the faradic oxidation/reduction reactions of Cu. The remaining 7.2 wt% of Cu was attributed to the mass of non-electroactive copper of the sample, considering 9.0 wt% of Cu obtained by ICP analysis. The contact between the material and the electrolyte on the remaining Cu did not exist. This was resulted from the morphology and size of Cu particles. It indicated that only Cu on the surface of the material took part in the electrochemical reactions.

3.2. Flammability of graphene based epoxy composites via LOI test

To examine the effect of graphenit-ox and graphenit-Cu on the flame retardant properties of epoxy composites, limiting oxygen index (LOI) test was performed. The effect on the flame retardant properties of epoxy composites with respect to the content of graphenit-ox and graphenit-Cu is depicted in Fig. 4. LOI values of 1% and 3% graphenit-ox-epoxy were 25.2 and 25.6%, respectively, which were a little higher than that of epoxy resin, 23.8%. It indicated that the addition of graphenit-ox did not effectively enhance the flame retardancy of epoxy resin. Nevertheless, LOI values of 1% and 3% graphenit-Cu-epoxy were reached to 25.8 and 26.4%, respectively (Fig. 4). The addition of graphenit-Cu slightly improved the flame retardancy of epoxy resin.

3.3. Combustion behaviors of graphene based epoxy composites via cone test

Cone calorimeter was utilized to study the flammability and potential fire safety of polymer-based materials under-ventilated conditions. This is one of the most effective bench-scale test

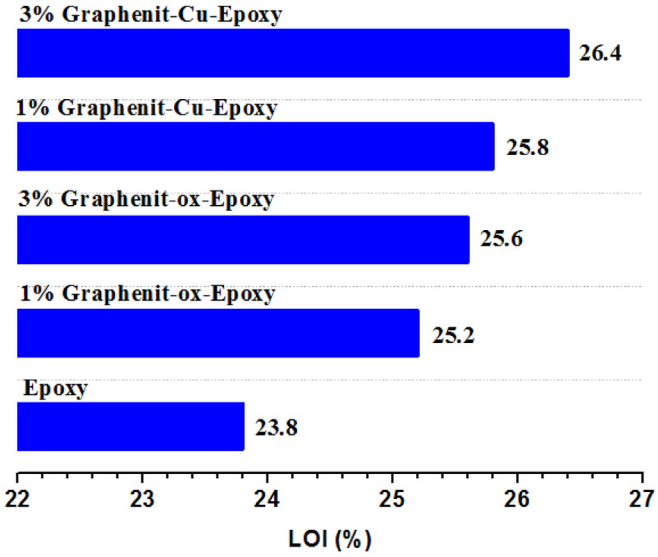

Fig. 4. LOI values of graphene based epoxy composites.

methods to predict the combustion behaviors of polymer-based materials in a real fire [3]. To examine the effect of graphenit-ox and graphenit-Cu on the combustion of epoxy composites, cone calorimeter test was performed. The important data acquired from the cone calorimeter test, such as time to ignition (TTI), peak heat release rate (PHRR), total heat release (THR), fire growth rate index (FIGRA, calculated from the ratio of PHRR and time to PHRR), time to PHRR (TPHRR), peak smoke production rate (PSPR), total smoke production (TSP) and residue, are presented in Table 1.

3.3.1. Heat release rate (HRR)

The HRR curves of epoxy composites with different contents of graphenit-ox and graphenit-Cu are shown in Fig. 5. Pure epoxy resin burned faster after ignition and a sharp peak appeared with a PHRR value of 1193 kW/m^2. Likewise, epoxy composites with 1% and 3% graphenit-ox also burned faster after ignition with the PHRR values of 1204 and 1244 kW/m^2, respectively, which were a little higher than that of pure epoxy resin. Thus, based on the results from LOI and cone tests, it was concluded the addition of graphenit-ox merely did not improve the flame retardant properties of epoxy composite. However, the PHRR values of epoxy composites with 1% and 3% graphenit-Cu were decreased to 825 and 786 kW/m^2, respectively, which were reduced by 31% and 34% compared with that of pure epoxy resin. This indicated that the flame retardant properties of epoxy composites were enhanced by the addition of graphenit-Cu into epoxy resin.

Further, there was an obvious delay in PHRR for epoxy composites with 1% and 3% graphenit-ox. In case of epoxy composites with 1% and 3% graphenit-ox, firstly, the heat release rate increased quickly, and then rose slowly, and again increased rapidly until it reached a maximum PHRR, and then gradually decreased. This phenomenon might be due to the formation of char layer. The formed char layer prevented the epoxy composites from both mass/heat transfer, showing the initial reduction in heat release. However, the char layer did not withstand at that higher temperature for a longer time. Not only that, the char layer may be fragile and cracked. Then, it might be busted that increased the heat release again.

The TTI value of epoxy composite with 1% graphenit-Cu was the same as that of pure epoxy resin (Fig. 5 and Table 1). There was an initial delay period for epoxy composites with different contents of

Table 1
Data obtained from cone test.

Sample	PHRR (kW/m^2) [%Reduction]	TPHRR[a] (s)	Av-HRR (kW/m^2)	TTI (s)	FIGRA (kW/m^2/s)	PSPR (m^2/s)	TSP (m^2)	THR (MJ/m^2) [%Reduction]	Mass (%)
Epoxy	1193 [–]	90	250	45	13.3	0.30	23	76 [–]	7.6
1%-Graphenit-ox-Epoxy	1204 [–1]	100	278	49	12.0	0.31	27	81 [–7]	12.9
3%-Graphenit-ox-Epoxy	1244 [–4]	90	341	47	13.8	0.39	25	72 [5]	14.1
1%-Graphenit-Cu-Epoxy	825 [31]	100	209	45	8.3	0.25	24	66 [13]	8.1
3%-Graphenit-Cu-Epoxy	786 [34]	110	220	47	7.1	0.25	23	64 [16]	11.0

[a] Note: TPHRR stands for time to PHRR.

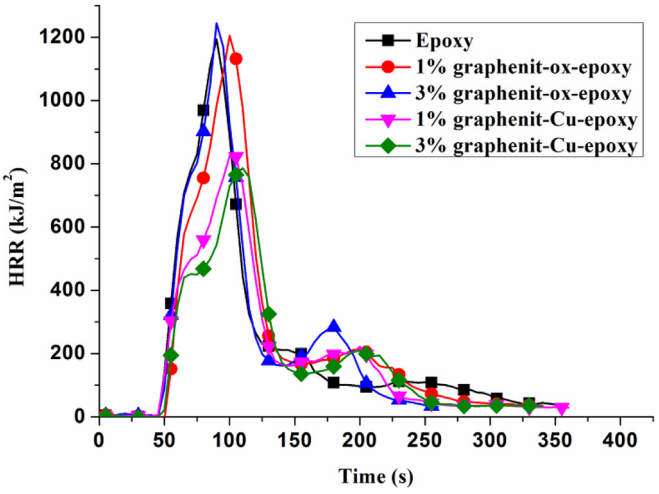

Fig. 5. HRR curves of graphene based epoxy composites.

graphenit-ox and graphenit-Cu before these composites started to release heat. The TTI values of these composites (47–49 s) were a little higher than that of neat epoxy resin, 45 s. And this suggested the addition of graphenit-ox improved the thermal degradation temperature of epoxy matrix. The FIGRA value of pure epoxy resin was 13.3 kW/(m^2 s), and for epoxy composites with different contents of graphenit-ox was 12.0 and 13.6 kW/(m^2 s). Interestingly, the FIGRA value for epoxy composites with different contents of graphenit-Cu was reduced to 8.3 and 7.1 kW/(m^2 s). The reduction in FIGRA revealed the suppression in fire spread in case of graphenit-Cu based epoxy composites.

3.3.2. Total heat release (THR)

THR curves of graphene based epoxy composites are presented in Fig. 6. At the end of burning, THR values for pure epoxy resin, epoxy composite with 1% graphenit-ox, epoxy composite with 3% graphenit-ox, epoxy composite with 1% graphenit-Cu and epoxy composite with 3% graphenit-Cu were 76, 81, 72, 66 and 64 kJ/m^2, respectively. Compared with pure epoxy resin, the addition of 1% graphenit-ox increased THR value of epoxy composites whereas the addition of graphenit-Cu decreased the THR values of epoxy composites. There were 13 and 16% reduction in THR value for epoxy composites with 1 and 3% graphenit-Cu, respectively (Fig. 6 and Table 1). Accordingly, the effect of graphenit-Cu was better than that of graphenit-ox on the flame retardant properties of epoxy composites.

3.3.3. Mass loss (ML)

ML curves of graphene based epoxy composites are presented in Fig. 7. At the end of burning, there were 7.6, 12.9, 14.1, 8.1 and 11.0% of char residue left, for pure epoxy resin, epoxy composite with 1% graphenit-ox, epoxy composite with 3% graphenit-ox, epoxy composite with 1% graphenit-Cu and epoxy composite with 3% graphenit-Cu, respectively. Compared to epoxy resin, the amount of char residue was increased with the addition of graphenit-ox (Fig. 7 and Table 1). So, the addition of graphenit-ox might promote the formation of more char residue from epoxy matrix. However, compared with those of epoxy composites with graphenit-ox, the addition of graphenit-Cu reduced the amount of char residue. It revealed the thermal degradation of epoxy matrix was accelerated with the addition of graphenit-Cu.

3.3.4. Smoke release

During a fire, total smoke production (TSP) and Smoke production rate (SPR) were the main cause of death [33]. Thus, the

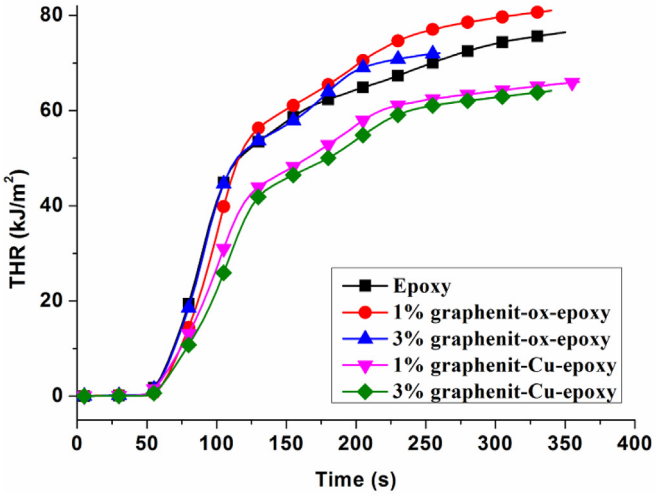

Fig. 6. THR curves of graphene based epoxy composites.

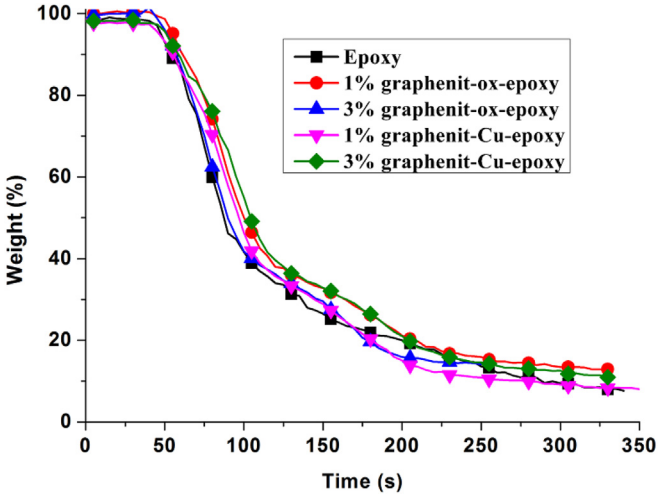

Fig. 7. ML curves of graphene based epoxy composites.

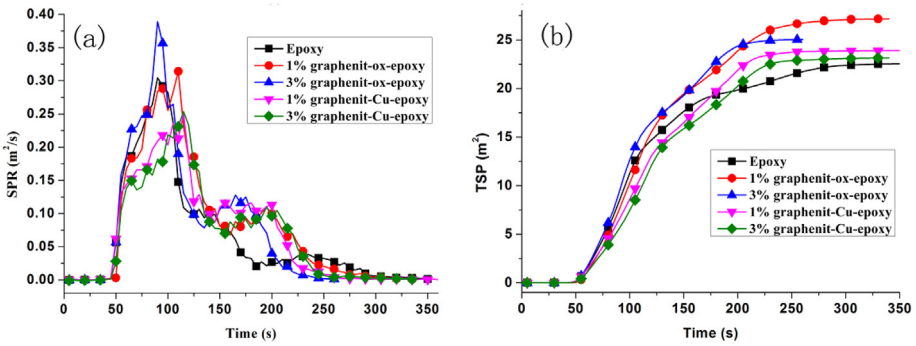

Fig. 8. SPR (a) and TSP (b) curves of graphene based epoxy composites.

investigation on TSP and SPR of polymeric materials was much beneficial in presenting the potential hazard of these materials [34]. TSP and SPR curves of graphene based epoxy composites are depicted in Fig. 8(a) and (b), respectively. Compared to pure epoxy resin, at the end of combustion, TSPs of graphene based epoxy composites were more than that of pure epoxy resin, and TSP decreased with the increase in the additive amount of graphenit-ox. This indicated that the addition of graphenit-ox led to the incomplete flammability of epoxy composites, releasing more amount of smoke. However, the addition of graphenit-Cu reduced the release of smoke, showing the reduction in TSP for epoxy composites; but, the TSP value of epoxy composite with 1% graphenit-Cu was still slightly higher than that of pure epoxy resin. The peak SPR (PSPR) values of graphene based epoxy composites were higher than that of pure epoxy during the flammability process, which were in agreement with TSP results (Fig. 8(b) and Table 1). However, the addition of graphenit-Cu decreased the PSPR of epoxy composites. Also the reduction in PSPR for epoxy composites with 1% and 3% graphenit-Cu were the same, 16.7%. Combined the analysis of LOI and cone tests of graphenit-ox and graphenit-Cu, it concluded that there might be a synergistic effect between graphene and Cu to retard the flame in epoxy composites.

3.4. Thermal degradation properties of graphene based epoxy composites

The effect of graphenit-ox and graphenit-Cu on the thermal degradation of epoxy composites was examined through TGA. TGA and DTG curves of graphene based epoxy composites are presented in Figs. 9 and 10, respectively; and the related data are shown in Table 2. All the TGA curves of graphene based epoxy composites were unimodal and displayed only one thermal degradation step in the experimental conditions (Figs. 9 and 10). This implied that the incorporation of graphenit-ox or graphenit-Cu into epoxy resin showed no significant effect on the thermal degradation mechanism of epoxy matrix. The addition of graphenit-ox had no obvious effect on the thermal degradation of epoxy composites and this was valid for all weight fractions (Fig. 9 and Table 2).

The onset degradation temperatures of epoxy composites with graphenit-ox, T_{onset}, defined as the temperature at which 5% mass loss took place, were slightly higher than that of pure epoxy resin. Compared with pure epoxy resin, there was almost no change in maximum decomposition temperature (T_{max}) for epoxy composites with graphenit-ox. The char yields of epoxy composites with graphenit-ox at 680 °C gradually rose with the increase of

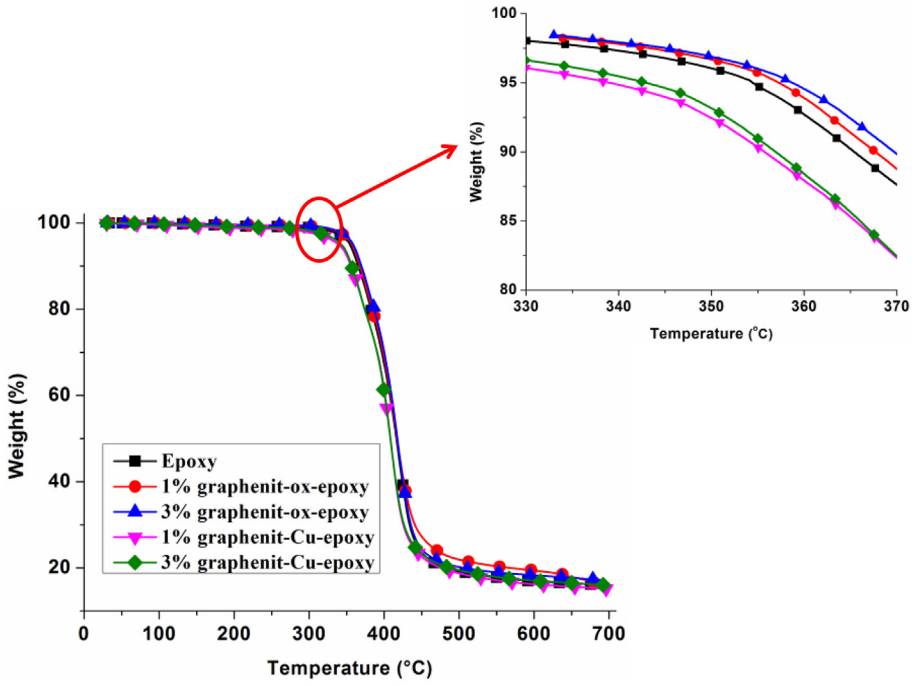

Fig. 9. TGA curves of graphene based epoxy composites.

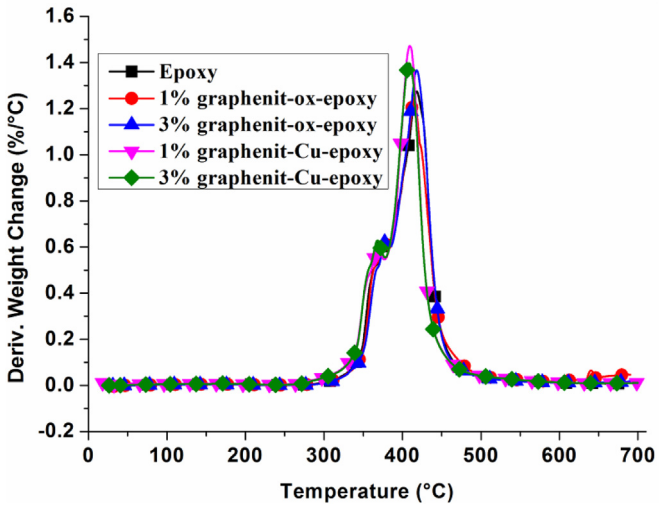

Fig. 10. DTG curves of graphene based epoxy composites.

graphenit-ox amount (Fig. 9 and Table 3). The char formed at this temperature was composed of epoxy and part of graphenit-ox. Thus, the addition of graphenit-ox did not promote the char formation of epoxy composite under nitrogen. However, the addition of graphenit-Cu decreased the T_{onset} of epoxy composite. The T_{onset}s of epoxy composites with 1% and 3% graphenit-Cu were decreased by 20 and 11 °C, respectively, and the T_{max}s were also reduced by 8 and 10 °C, respectively, with the addition of graphenit-Cu. The results revealed that the addition of graphenit-Cu accelerated the thermal degradation of epoxy composites, provided less amount of char residue in epoxy composites and released more amounts of gases.

The addition of graphenit-ox slightly reduced the thermal degradation rate at T_{max}s of epoxy composite whereas the addition of graphenit-Cu increased the thermal degradation rate at T_{max}s of epoxy composites when compared with pure epoxy resin (Fig. 10 and Table 2). This also indicated that the addition of graphenit-Cu might promote the thermal degradation of epoxy composite to release more amounts of inflammable gases, leading to an enhancement of flame retardancy of epoxy composites.

3.5. Dynamic mechanical analysis (DMA) of graphene based epoxy composites

Dynamic mechanical test was very sensitive to chemical and physical structure of polymeric materials. It was studied to examine about the morphology and glass transitions of polymeric materials [35]. The effect of temperature on storage modulus and loss factor tan δ of graphene based epoxy composites with different additive amounts of graphenit-ox and graphenit-Cu are displayed in Fig. 11. The storage modulus in glassy and rubbery state, and glass transition temperature (T_g, obtained from tan δ peak) are listed in Table 3. The addition of graphenit-ox and graphenit-Cu reduced the storage

Table 2
Data obtained from TGA and DTG curves of graphene based epoxy composites.

Sample	T_{onset} (°C)	T_{max} (°C)	R_{max} (%/°C)	Residue (%)		
				500 °C	600 °C	680 °C
Epoxy	354	419	1.3	19.2	16.9	16.2
1%-Graphenit-ox-Epoxy	357	415	1.2	21.9	19.4	16.7
3%-Graphenit-ox-Epoxy	359	418	1.4	20.2	18.3	17.3
1%-Graphenit-Cu-Epoxy	334	411	1.5	18.7	16.2	15.3
3%-Graphenit-Cu-Epoxy	343	409	1.4	19.5	17.0	16.2

Table 3
Data obtained from DMA test.

Sample	Storage Modulus (E'_g) at 30 °C (Mpa)	Rubbery Modulus (E'_r) at 200 °C (Mpa)	T_g (°C)
Epoxy	2367	17	171
1%-Graphenit-ox-Epoxy	2148	24	170
3%-Graphenit-ox-Epoxy	2254	27	168
1%-Graphenit-Cu-Epoxy	2280	25	176
3%-Graphenit-Cu-Epoxy	2223	28	176

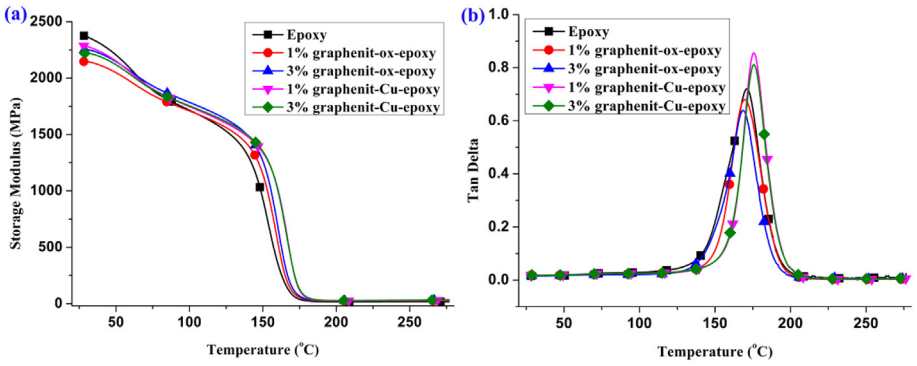

Fig. 11. Storage modulus (a) and tan δ (b) curves of graphene based epoxy composites.

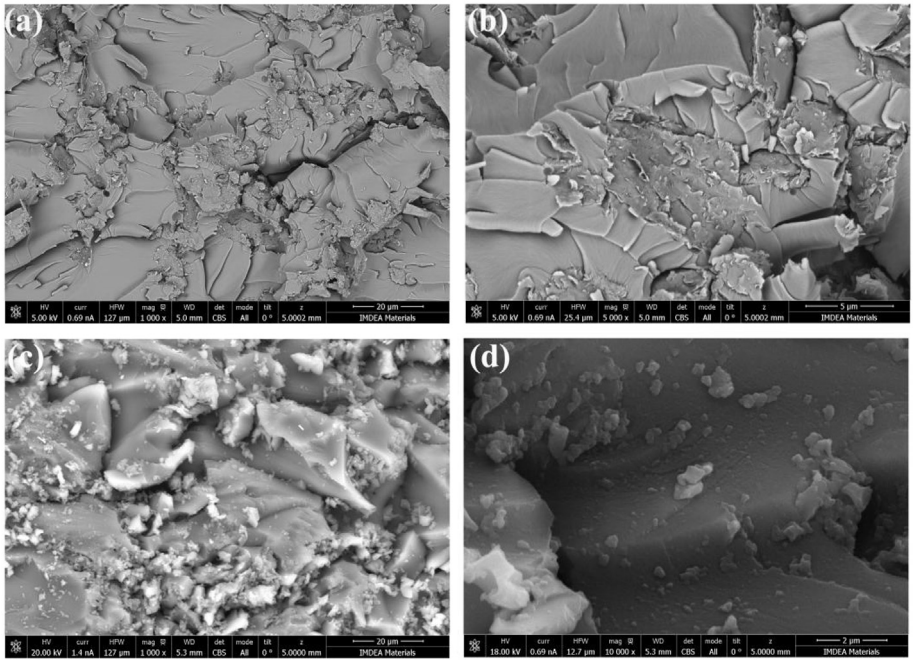

Fig. 12. FIB-FEGSEM pictures of 3% graphenit-ox epoxy composites (a, b) and 3% graphenit-Cu epoxy composites (c, d).

modulus values of epoxy composites at lower temperature (<61 °C), compared to pure epoxy resin (Fig. 11(a)). These results might result from the bad disperse state of graphenit-ox (or graphenit-Cu) in epoxy resin. In order to observe the disperse state of graphenit-ox (or graphenit-Cu) in epoxy resin, a focused ion beam-field emission gun scanning electron microscope (FIB-FEGSEM) was utilized. FIB-FEGSEM pictures of epoxy composites with 3% graphenit-ox and epoxy composites with 3% graphenit-Cu were depicted in Fig. 12. From Fig. 12, it can be observed that the cross-section of epoxy composites was quite rough, indicating that the compatibility between graphenit-ox (or graphenit-Cu) and epoxy resin was not good. The particle size of graphenit-ox (or graphenit-Cu) (shown in Fig. 1) used in this study was quite bigger, and the oxidized degree of graphenit-ox was slightly, which might the reason for the bad compatibility. However, from Fig. 11(a) and Table 3, it was noted that the storage modulus value of epoxy composites with 3% graphenit-ox, 2254 MPa, was higher than that of epoxy composites with 1% graphenit-ox, 2148 MPa, at 30 °C. This phenomenon might be resulted from the interfacial interactions between graphenit-ox and epoxy resin. In the case of epoxy composites with 3% graphenit-ox, there existed more amounts of hydroxyl and epoxy groups obtained from graphenit-ox, and these groups reacted with epoxy resin, resulting in the better disperse state of graphenit-ox in epoxy resin. As can be obtained from Fig. 11(a) and Table 3, the storage modulus value at 30 °C of epoxy composites with 1% graphenit-Cu was higher than that of epoxy composites with 1% graphenit-ox. The doped copper might catalyze the chemical reactions between grapheme and epoxy resin, improving the compatibility of graphenit-Cu and epoxy resin. Moreover, the storage modulus values of graphene based epoxy composites were higher than the corresponding value of pure epoxy resin at higher temperature (>85 °C). Mohanty et al. [36] had reported the similar results for epoxy/20% EMS/C30B nanocomposite. This behavior might be due to the higher crosslinked density, and the increase in the stiffness of polymeric materials were caused by well dispersed graphenit-ox (or graphenit-Cu) [37]. A rheological percolation might be achieved in graphene based epoxy composites. And the formed percolated network of graphene reduced the mobility of epoxy chains at higher temperature [38].

The loss factor tan δ curves of graphene based epoxy composites are presented in Fig. 11(b). The addition of graphenit-ox reduced T_gs of epoxy composites (Fig. 11(b) and Table 3). Graphenit-ox (slightly oxidized graphene nanoplatelets) had lower oxygen levels and thus it should have weaker interactions at the interfaces with epoxy resin due to the lack of hydroxyl and epoxy groups [39]. However, it was interesting to note that T_gs of epoxy composites with 1% and 3% graphenit-Cu were increased by 5 °C compared to pure epoxy resin. And this indicated that the addition of graphenit-Cu restricted the mobility of epoxy chains and increased the cross-linking density of epoxy composites. Higher T_gs of epoxy composites with graphenit-Cu also indicated a stronger bonding and load transfer at the graphenit-Cu-epoxy interface [38]. Compared to pure epoxy resin, the E'_r values of graphene based epoxy composites were much higher, which showed the stronger interaction between graphenit-ox (graphenit-Cu) and epoxy matrix, and the higher crosslinking degree of epoxy composites [38].

4. Conclusions

Graphenit-ox/epoxy and graphenit-Cu/epoxy composites were successfully prepared and thoroughly characterized using standard analytical techniques. LOI value of epoxy composite with 3% graphenit-ox was improved to 25.8% from 23.8% for pure epoxy resin whereas LOI value of epoxy composite with 3% graphenit-Cu was enhanced to 26.4%. The cone results revealed that the addition of graphenit-Cu reduced the heat release rate (HRR), total smoke production (TSP) and smoke production rate (SPR) of epoxy composites; however, the addition of graphenit-ox had little flame retardant effect on epoxy composites. There might be a synergistic effect between graphene and Cu on the flame retardant epoxy composites. TGA and DMA results indicated that the addition of graphenit-ox had slight effect on the thermal degradation and thermomechanical properties of epoxy composites; however, the addition of graphenit-Cu accelerated the thermal degradation of

epoxy composites and increased the glass transition temperature (T_g) of epoxy composites.

Acknowledgment

The authors acknowledged the financial support of China Scholarship Council (CSC: 201308420380), National Natural Science Foundation of China (Grant No. U1201243) and the European Union's Seventh Framework Program for Research, Technological Development and Demonstration (607793). This research is also partly supported by Spanish Ministry of Economy and Competitiveness (MINECO) under Ramón y Cajal grant (RYC-2012-10737).

References

[1] Wang JS, Liu Y, Zhao B, Liu J, Wang DY, Song YP, et al. Metal compound-enhanced flame retardancy of intumescent epoxy resins containing ammonium polyphosphate. Polym Degrad Stab 2009;94:625–31.
[2] Wang X, Hu Y, Song L, Xing WY, Lu HD, Lv P, et al. Flame retardancy and thermal degradation mechanism of epoxy resin composites based on a DOPO substituted organophosphorus oligomer. Polymer 2010;51:2435–45.
[3] Gao LP, Wang DY, Wang YZ, Wang JS, Yang B. A flame-retardant epoxy resin based on a reactive phosphorus-containing monomer of DODPP and its thermal and flame-retardant properties. Polym Degrad Stab 2008;93:1308–15.
[4] Sahoo SK, Mohanty S, Nayak SK. Effect of lignocellulosic fibers on mechanical, thermomechanical and hydrophilic studies of epoxy modified with novel bioresin epoxy methyl ester derived from soybean oil. Polym Adv Tech 2015;26:1619–26.
[5] Zhao W, Liu JP, Peng H, Liao JY, Wang XJ. Synthesis of a novel PEPA-substituted polyphosphoramide with high char residues and its performance as an intumescent flame retardant for epoxy resin. Polym Degrad Stab 2015;118:120–9.
[6] Im JS, Lee SK, In SJ, Lee YS. Improved flame retardant properties of epoxy resin by fluorinated MMT/MWCNT additives. J Anal Appl Pyrol 2010;89:225–32.
[7] Guo YQ, Bao CL, Song L, Yuan BH, Hu Y. In situ polymerization of graphene, graphite oxide, and functionalized graphite oxide into epoxy resin and comparison study of on-the-flame behavior. Ind Eng Chem Res 2011;50:7772–83.
[8] Liao SH, Liu PL, Hsiao MC, Teng CC, Wang CA, Ger MD, et al. One-step reduction and functionalization of graphene oxide with phosphorus-based compound to produce flame-retardant epoxy nanocomposite. Ind Eng Chem Res 2012;51:4573–81.
[9] Wang X, Hu Y, Song L, Xing WY, Lu HD. Thermal degradation behaviors of epoxy resin/POSS hybrids and phosphorus-silicon synergism of flame retardancy. J Polym Sci Pol Phys 2010;48:693–705.
[10] Li KY, Kuan CF, Kuan HC, Chen CH, Shen MY, Yang JM, et al. Preparation and properties of novel epoxy/graphene oxide nanosheets (GON) composites functionalized with flame retardant containing phosphorus and silicon. Mater Chem Phys 2014;146:354–62.
[11] Dogan M, Unlu SM. Flame retardant effect of boron compounds on red phosphorus containing epoxy resins. Polym Degrad Stab 2014;99:12–7.
[12] Wang X, Hu Y, Song L, Xing WY, Lu HD. Preparation, flame retardancy, and thermal degradation of epoxy thermosets modified with phosphorous/nitrogen-containing glycidyl derivative. Polym Adv Tech 2012;23:190–7.
[13] Mercado LA, Galià M, Reina JA. Silicon-containing flame retardant epoxy resins: synthesis, characterization and properties. Polym Degrad Stab 2006;91:2588–94.
[14] Liu H, Wang XD, Wu DZ. Novel cyclotriphosphazene-based epoxy compound and its application in halogen-free epoxy thermosetting systems: synthesis curing behaviors and flame retardancy. Polym Degrad Stab 2014;103:96–112.
[15] Kandare E, Kandola BK, Staggs JEJ. Global kinetics of thermal degradation of flame-retarded epoxy resin formulations. Polym Degrad Stab 2007;92:1778–87.
[16] Lee SK, Bai BC, Im JS, In SJ, Lee YS. Flame retardant epoxy complex produced by addition of montmorillonite and carbon nanotube. J Ind Eng Chem 2010;16:891–5.
[17] Zotti A, Borriello A, Ricciardi M, Antonucci V, Giordano M, Zarrelli M. Effects of sepiolite clay on degradation and fire behavior of a bisphenol A-based epoxy. Compos Part B Eng 2015;73:139–48.
[18] Kalali EN, Wang X, Wang DY. Functionalized layered double hydroxide-based epoxy nanocomposites with improved flame retardancy and mechanical properties. J Mater Chem A 2015;3:6819–26.
[19] Li C, Wan JT, Kalali EN, Fan H, Wang DY. Synthesis and characterization of functional eugenol derivative based layered double hydroxide and its use as nano flame-retardant in epoxy resin. J Mater Chem A 2015;3:3471–9.
[20] Wang X, Kalali EN, Wang DY. Renewable cardanol-based surfactant modified layered double hydroxide as a flame retardant for epoxy resin. ACS Sus Chem Eng 2015;3:3281–90.
[21] Wang FZ, Drzal LT, Qin Y, Huang ZX. Processing and characterization of high content multilayer graphene/epoxy composites with high electrical conductivity. Polym Compos 2015. http://dx.doi.org/10.1002/pc.23487.
[22] Wang ZH, Wei P, Qian Y, Liu JP. The synthesis of a novel graphene-based inorganic-organic hybrid flame retardant and its application in epoxy resin. Compos Part B Eng 2014;60:341–9.
[23] Kim H, Abdala AA, Macosko CW. Graphene/Polymer nanocomposites. Macromolecules 2010;43:6515–30.
[24] Liu F, Hu N, Ning HM, Liu YL, Li Y, Wu LK. Molecular dynamics simulation on interfacial mechanical properties of polymer nanocomposites with wrinkled graphene. Comput Mater Sci 2015;108:160–7.
[25] Zhao YH, Wu ZK, Bai SL. Study on thermal properties of graphene foam/graphene sheets filled polymer composites. Compos Part A Appl Sci 2015;72:200–6.
[26] Dittrich B, Wartig KA, Hofmann D, Mülhaupt R. Flame retardancy through carbon nanomaterials: carbon black, multiwass nanotubes, expanded graphite, multi-layer graphene and graphene in polypropylene. Polym Degrad Stab 2013;98:1495–505.
[27] Huang GB, Chen SQ, Tang SW, Gao JR. A novel intumescent flame retardant-functionalized graphene: nanocomposite synthesis, characterization, and flammability properties. Mater Chem Phys 2012;135:938–47.
[28] Pour RH, Soheilmoghaddam M, Hassan A, Bourbigot S. Flammability and thermal properties of polycarbonate/acrylonitrile-butadiene-styrene nanocomposites reinforced with multilayer graphene. Polym Degrad Stab 2015;120:88–97.
[29] Zhang K. Fabrication of copper nanoparticles/graphene oxide composites for surface-enhanced Raman scattering. Appl Surf Sci 2012;258:7327–9.
[30] Fukunaga T, Nagano K, Mizutani U, Wakayama H, Fukushima Y. Structural change of graphite subjected to mechanical milling. J Non-Cryst Solids 1998;232–234:416–20.
[31] Diaz-Droguett DE, Espinoza R, Fuenzalida VM. Copper nanoparticles grown under hydrogen: study of the surface oxide. Appl Surf Sci 2011;257:4597–602.
[32] Jayalakshmi M, Balasubramanian K. Cyclic voltammetric behavior of copper powder immobilized on paraffin impregnated graphite electrode in dilute alkali solution. Int J Electrochem Sci 2008;3:1277–87.
[33] Liu Y, Zhao J, Deng CL, Chen L, Wang DY, Wang YZ. Flame-retardant effect of sepiolite on an intumescent flame-retardant polypropylene system. Ind Eng Chem Res 2011;50:2047–54.
[34] Wang DY, Liu Y, Ge XG, Wang YZ, Stec A, Biswas B, et al. Effect of metal chelates on the ignition and early flaming behavior of intumescent fire-retarded polyethylene systems. Polym Degrad Stab 2008;93:1024–30.
[35] Gabr MH, Phong NT, Okubo K, Uzawa K, Kimpara I, Fujii T. Thermal and mechanical properties of electrospun nano-celullose reinforced epoxy nanocomposites. Polym Test 2014;37:51–8.
[36] Sahoo SK, Mohanty S, Nayak SK. A study on effect of organo modified clay on curing behavior and thermo-physical properties of epoxy methyl ester based epoxy nanocomposite. Thermochim Acta 2015;614:163–70.
[37] Miyagawa H, Mohanty AK, Burgueno R, Drzal LT, Misra M. Characterization and thermophysical properties of unsaturated polyester-layered silicate nanocomposites. J Nanosci Nanotechnol 2006;6:464–71.
[38] Chandrasekaran S, Seidel C, Schulte K. Preparation and characterization of graphite nano-platelet (GNP)/epoxy nano-composite: mechanical, electrical and thermal properties. Eur Polym J 2013;49:3878–88.
[39] Liao KH, Aoyama S, Abdala AA, Macosko C. Does graphene change T_g of nanocomposites. Macromolecules 2014;47:8311–9.